Applied Surface Science 257 (2011) 2474–2480

Contents lists available at ScienceDirect

Applied Surface Science

journal homepage: www.elsevier.com/locate/apsusc

Configuration and electronic properties of graphene nanoribbons on Si(2 1 1) surface

W. Wang, L.Z. Sun*, C. Tang, X.L. Wei, J.X. Zhong

Laboratory for Quantum Engineering and Micro-Nano Energy Technology, Xiangtan University, Yuhu Road, Xiangtan 411105, Hunan, China

ARTICLE INFO

Article history:
Received 12 February 2010
Received in revised form
27 September 2010
Accepted 1 October 2010
Available online 23 October 2010

Keywords:
Si(2 1 1) surface
GNRs
Adsorption
Electronic structure

ABSTRACT

We perform first-principles calculations based on density functional theory to study the configuration and electronic properties of graphene nanoribbons (GNRs) on Si(2 1 1) surface. Both [0 1 $\bar{1}$] and [$\bar{1}$ 1 1] adsorption orientations of Si(2 1 1) surface are considered. We find that the adsorption energy is determined not only by the edge states of GNRs, but also by the ribbon width and the orientation of the substrate. Bridge and M-shape adsorption configurations appear gradually as the ribbon width increases. The substrate effectively affects the edge states of GNRs and tends to depress the metallic nature of zigzag GNRs (Z-GNRs) and metallize the armchair GNRs (A-GNRs).

1. Introduction

Graphene nanoribbons (GNRs) [1–3], quasi-one-dimensional materials can be patterned from graphene, have recently attracted intense interest as a fascinating building block for nano-electronic and spintronic devices due to their unique transport properties [4] and electronic structure [5–7]. Moreover, their transport properties and electronic structure can be modulated by their chirality, geometry or chemical modification. For example, the H-passivated zigzag GNRs (Z-GNRs) are metallic, whereas the H-passivated armchair GNRs (A-GNRs) show metallic or semiconducting nature depending on their ribbon width [8]. Lots of prototypic devices, such as field effect transistors, have been proposed [9] and fabricated [10] by the GNRs. The interaction between graphene/GNRs and substrate has also drawn a great deal of attention. Mattausch et al. [11] and Varchon et al. [12] reported the adsorption of graphene on SiC. However, they found that the graphene adsorbed on SiC surface does not exhibit the nature of single-layer graphite film until add up to two or multiple layers. Sorkin et al. [13] reported that on the Si-terminated SiC(0 0 0 1) surface the initial planar shape of GNRs is substantially distorted by the underlying substrate, however, as for the C-terminated SiC(0 0 0 1) substrates the planar shape of GNRs reserves. Zhang et al. [14] found that the electronic properties of Z-GNRs adsorbed on Si(0 0 1) substrate strongly depend on their ribbon width and adsorption orientation.

In view of the important role of the silicon material in the future nano-technology, the combination of GNRs and silicon is a significant issue for the practical applications of GNRs. There are a lot of experimental and theoretical studies for the adsorption of materials on the silicon substrate [15–19]. However, to our knowledge, the theoretical studies on the interaction between GNRs and the silicon substrate are few. Moreover, the stability and electronic properties of GNRs adsorbed on Si(2 1 1) surface has not been reported as yet. The main purpose of this paper is to explore the adsorption configuration and electronic structure of GNRs adsorbed on Si(2 1 1) substrate. The main reason we choose the Si(2 1 1) surface is that it is a High-Miller-index surface with step reconstruction [20]. The nature of the surface can efficiently modulate the structure and the electronic properties of GNRs adsorbed on it. In our present paper, we find that the stability of GNRs on the Si(2 1 1) surface is mainly determined by the sp^3 hybridization between the edge carbon atoms of GNRs and the silicon atoms of the substrate. Consequently, the adsorption energy of GNRs on the surface relies on the ribbon width and the orientation of the substrate. We also find that the substrate tends to depress the metallic nature of Z-GNRs and metallize the A-GNRs.

2. Computational details

The structures of Z-GNRs and A-GNRs are shown in Fig. 1a and b. N_z and N_a (here we adopt the nomenclature of reference [21]) denote the number of zigzag carbon chains and carbon dimer lines of Z-GNRs and A-GNRs, respectively. In our present work, in order to keep the ribbon width increasing by a complete honey-

* Corresponding author. Tel.: +86 731 5829199.
E-mail addresses: lzsun@xtu.edu.cn (L.Z. Sun), jxzhong@xtu.edu.cn (J.X. Zhong).

0169-4332/$ – see front matter © 2010 Elsevier B.V. All rights reserved.
doi:10.1016/j.apsusc.2010.10.004

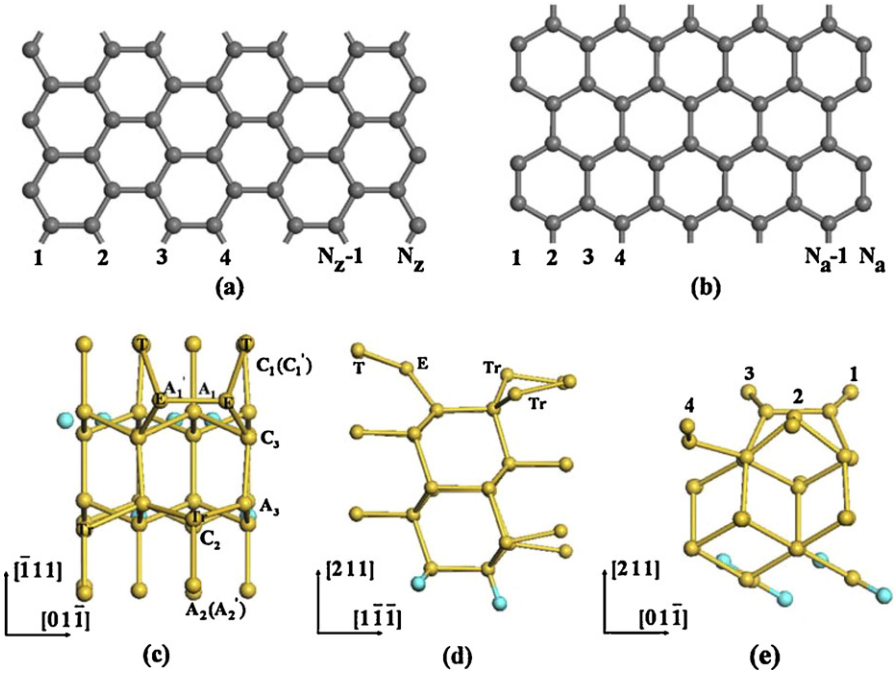

Fig. 1. Schematic diagram of the structures for Z-GNRs (a), A-GNRs (b) and top view of Si(2 1 1) unit cell (c), respectively. (d and e) Two different side views of Si(2 1 1) unit cell. Gray, yellow and blue balls represent carbon, silicon and hydrogen atom, respectively. (For interpretation of the references to color in this figure legend, the reader is referred to the web version of the article.)

combs gradually, the number of N_z increases from 4 to 13 by 1 and N_a increases from 7 to 23 by 2. The width is in the range of 7.10–26.28 Å and 7.38–27.06 Å for Z-GNRs and A-GNRs, respectively. Both H-terminated and H-free GNRs are considered here because they have different electronic properties. Fig. 1c–e shows the top view and two different orientated side views of the unit cell of Si(2 1 1) surface. The marked symbols of the bond lengths and the bond angles of the surface adopted from the report of Grein et al. [22]. The optimized bond lengths and the bond angles of the surface (the computational details as follows) are summarized in Table 1. The optimized reconstruction configuration of Si(2 1 1) is in agreement with the report of Grein et al. [22] to some extent. All optimized bond lengths and the bond angle of C_1–A_1–A_1' differ from Grein's within 3.50% and 0.60%, respectively. However, in comparison with the structure reported by Grein et al. [22], the bond angles of C_1–A_1–C_3 and A_1–C_3–A_3 are enlarged up to 19.15% and 7.66%, and the bond angle of A_2'–C_1–A_1 is lessened 7.53%, respectively. The deflection mainly derives from the different methods between Grein's and ours.

Based on the two dimensional (2×1) reconstructed Si(2 1 1) surface unit cell obtained above, we extend it 4 times along the [$\bar{1}$ 1 1] direction and 5 times along the [0 1 $\bar{1}$] direction to build up the 4×1 and 1×5 supercells, respectively. The 4×1 and 1×5 supercells are corresponding to the adsorption orientation of [0 1 $\bar{1}$] and [$\bar{1}$ 1 1], respectively. 9 and 7 monolayers are chosen for the 4×1 and 1×5 supercells, respectively. The dangling bonds of silicon atoms at the bottom layer are passivated by hydrogen, and two adjacent image surfaces are separated by a vacuum region around 10–13 Å. The existence of lattice mismatch between GNRs and silicon substrate is inevitable. To reduce the lattice mismatch, we stretch or contract the lattice of the GNRs and the surface trivially. Such adjustments of the lattice may affect the absolute results of each system, but it does not affect the evolution of the adsorption stability and the electronic structure emphasized in our present work. The computational model in our present work is a slab with two surfaces embedded with vacuum regions in a supercell imposed periodic boundary conditions. The dipole correction for such supercell should be considered. However, as for our present model, the slab as shown in Fig. 1 is not a polarized system. The dipole creates by the electrostatic potential between the periodic slabs is typically small. We have used the dipole correction method introduced by Neugebauer et al. [23] test several cases of our models, the dipole correction only slightly affects the adsorption configurations. Moreover, though such correction influences the absolute total energy of each systems, the relative one, namely the adsorption energy derived from the difference between two systems, is unchanged. In view of such validation, the dipole correction is not considered in our present work.

Our calculations are performed with the density functional package VASP [24–26]. Ionic potentials are represented by projected augmented wave (PAW) [27], and the exchange correlation potential is described with generalized gradient approximations-PBE functional [28]. In our present work, the largest supercell contains 269 atoms. The plane-wave cutoff energy is chosen as 400 eV. Brillouin zone integrations are performed with Gaussian broadening [29] of 0.1 eV. The Brillouin zone is sampled by using $1 \times 1 \times 1$ Gamma centered Monkhorst-Pack grids for the calculations of relaxation. Gamma centered grids with $1 \times 3 \times 1$ and

Table 1
Coefficients of Si(2 1 1) surface. The units of bond length and bond angle are angstrom (Å) and degree(°), respectively. Δd is the change ratio between ours and the results from the previous work [22].

Atoms	Previous work (Ref. [19])	Present work	Δd
C_1–A_1	2.33	2.26	−3.13%
A_1–A_1'	2.39	2.34	−2.09%
A_1–C_3	2.39	2.31	−3.35%
C_3–A_3	2.37	2.36	−0.34%
A_3–C_2	2.32	2.38	2.46%
C_2–A_2	2.33	2.37	1.68%
A_2–C_1'	2.35	2.37	0.69%
A_2'–C_1–A_1	94.3	87.2	−7.53%
C_1–A_1–C_3	108.1	128.8	19.15%
C_1–A_1–A_1'	107.2	107.8	0.59%
A_1–C_3–A_3	112.0	120.6	7.66%